Production of d^* dibaryon in proton-deuteron collisions

A. B. Santra,[1] B. K. Jain,[1] and V. S. Bhasin[2]
[1]*Nuclear Physics Division, Bhabha Atomic Research Centre, Mumbai 400 085, India*
[2]*Physics Department, Delhi University, Delhi 110 007, India*
(Received 18 October 2001; published 4 March 2002)

We have studied the excitation mechanism of d^*, a bound state of two deltas (Δ), in proton-deuteron collisions. In our model for the mechanism of d^* excitation in this reaction, the incident proton interacts with both nucleons of the deuteron, exciting each one of them to the Δ state in sequence. The $V_{NN\to N\Delta}$ transition potential is described by the one-pion exchange, parameters of which are fixed taking guidance from studies on $pp\to N\Delta$ reaction. The results presented here are for angular distribution, mass distribution, t distribution, and the excitation function. We find that the position of the peak in the mass distribution is directly related to the strength of the $\Delta-\Delta$ binding potential. The excitation function peaks between 300- and 550-MeV beam energy for binding potentials between 500 and 350 MeV. The angular distribution peaks around 55°–60°.

DOI: 10.1103/PhysRevC.65.034012 PACS number(s): 21.30.−x, 21.45.+v, 25.40.Ny

I. INTRODUCTION

The strongly interacting systems such as baryons, mesons, nuclei, and neutron star, which have been observed so far, comprise only a fraction of the wide range of particles and systems that may exist with quarks and gluons as building blocks. Other strongly interacting systems include exotic quark-gluon systems, strangelets, strange star, and quark-gluon plasma. Experimental search for these new systems is being carried out for a long time. It is believed that the study of these exotic systems will help in understanding that part of the strong interaction that has not yet been possible to calculate from the first principles using QCD.

Among the exotic quark-gluon systems, let us consider the dibaryons. The stable dibaryon system is deuteron. Its properties are well understood [1,2] in terms of a nonrelativistic description of two-body system with meson-exchange nucleon-nucleon interacting potentials. However, there are other dibaryon resonances. As early as 1977, Jaffe [3] predicted the existence of a dibaryon in the strange sector (di-hyperon), called H particle, which is yet to be observed experimentally, though its presence at the core of neutron stars has been talked about [4]. The other promising candidate is d^* dibaryon [5] having quantum numbers, $J^\pi T=3^+0$. This dibaryon is a six-quark state with quark-exchange symmetry such that at large interbaryon separation it has the behavior of a pair of Δ's. Considering that the production cross section for a Δ in the hadronic collisions at intermediate energies is large, production of d^* through $\pi d\to pd^*$ and using proton beams should have good cross sections. Model estimates exist in the literature [6,7] for these cross sections. With the availability of high-quality electron beams, electroproduction of dibaryon resonances also looks promising and studies [8,9] have been made for d^* electroproduction cross section. Indiana group [10] has suggested the possibility of d^* observation via $d(\vec{d},\vec{d}')$ reaction.

In the last few years, after Bilger *et al.* [11] reported on the observation of narrow dibaryon state of mass 2.06 GeV, a large number of experiments [12–22] devoted to the search of dibaryon resonance d^* have been done. Despite these efforts, the existence or nonexistence of d^* has not been established yet.

As regards the short-range behavior of the interaction between two Δ's, there are many QCD inspired models for describing hadronic interactions. These models differ from each other in the choice of degrees of freedom and in giving importance to one or the other feature (confinement or chiral symmetry) of QCD. All these models are equally good or bad in describing the hadron spectroscopy and the existing data of hadron interactions. It is difficult to discriminate one model from the other. One common feature of all these models, however, is that they predict a binding potential of varying depth for two Δ's in $T=0$ and $S=3^+$ states. Therefore, observation of the d^* dibaryon state will have implications on these models particularly in knowing the depth and range of the interaction potential.

In this paper we calculate various cross sections of $pd\to pd^*$ reaction. In our calculations we do not make any reference to quark structure of baryons. We use hadronic degrees of freedom only. The t matrix for $pN\to N\Delta$ transition is taken as the one that describes the existing data on the Δ production in p-p collisions. The d^* bound-state wave function is generated in a square well potential with varying depth. For the deuteron wave function we have taken a simple form of Hulthen wave function.

The paper is organized as follows. We discuss the excitation mechanism of the d^* dibaryon in Sec. II, and write the mass distribution function of d^* in Sec. III. The transition matrix for $pd\to pd^*$ is constructed in Secs. IV, V, and VI, which gives bound-state wave functions for deuteron and d^* and the expressions for various cross sections, respectively. The results are discussed in Sec. VII and a summary is given in Sec. VIII.

II. d^* EXCITATION MECHANISM

The d^* dibaryon is a spin 3^+ state. So, the dominant hadron component of it is $\Delta\Delta$. Its isospin is zero ($T=0$). The isospin part of d^* wave function, hence, can be written as

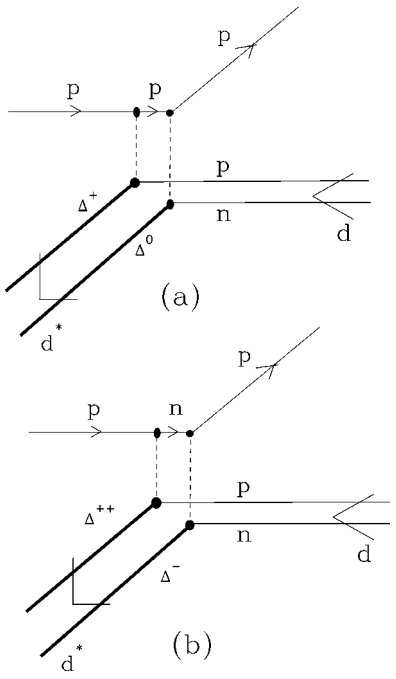

FIG. 1. Schematic diagram of the direct process of $pd \rightarrow pd^*$.

$$d^* = \frac{1}{2}[|\Delta^{++}\Delta^{-}\rangle - |\Delta^{+}\Delta^{0}\rangle + |\Delta^{0}\Delta^{+}\rangle - |\Delta^{-}\Delta^{++}\rangle]. \qquad (1)$$

To produce a d^* dibaryon from a nuclear target it is necessary to change two nucleons to two Δ's. In case of a simple nuclear target, e.g., deuteron, it is achieved by the incoming proton interacting successively with both the nucleons of the deuteron and converting them into Δ's. Specifically, as shown in Fig. 1, the beam proton interacts with the proton in the deuteron and converts it into Δ^+ and then propagates and interacts with the neutron and converts it into Δ^0. Alternatively, while interacting with the proton in the deuteron the beam proton gets charge exchanged with a neutron and the proton in the target gets excited to Δ^{++}. This neutron at the second stage, while interacting with the target neutron, again gets charge exchanged with the proton and excites the target neutron to Δ^-. These two diagrams, thus, produce the $|\Delta^+\Delta^0\rangle$ and $|\Delta^{++}\Delta^-\rangle$ components of the d^*.

We show in Fig. 2 another possibility of d^* excitation. In Fig. 2(a), the incident proton while interacting for the second time gets bound to Δ^0 (formed from the neutron of deuteron after the first interaction) converting itself to Δ^+ and the proton from the deuteron goes to the continuum. In Fig. 2(b), the neutron of the intermediate state gets bound to Δ^{++} (formed from the proton of deuteron after the first interaction) converting itself to Δ^- and the neutron of the deuteron goes to the continuum after converting itself to proton. We call the diagrams of Fig. 2 as exchange diagrams whereas those of Fig. 1 as direct diagrams. We have restricted ourselves only to diagrams with vertices having two nucleons or one nucleon and one Δ without considering vertices with two Δ's. Actually, we get eight diagrams in total; four more diagrams are obtained by exchanging neutron and proton lines of deuteron in Figs. 1 and 2.

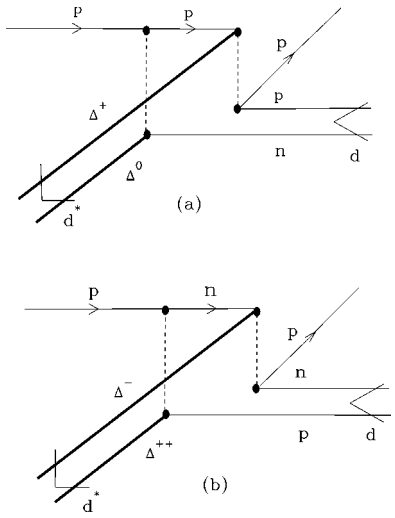

FIG. 2. Schematic diagram of $pd \rightarrow pd^*$.

The transition amplitude for $pd \rightarrow pd^*$ is thus constructed taking coherent sum of the contributions coming from each diagram with appropriate phase factor.

III. MASS DISTRIBUTION OF d^*

The mass of d^* is not fixed but distributed over a range, as it is made of two Δ's that are unstable particles. The mass distribution function $\rho_{d^*}(\mu)$ of d^* can be constructed as a convolution of the mass distribution functions of its two constituent Δ's as

$$\rho_{d^*}(\mu) = \int \rho_\Delta(\mu')\rho_\Delta(\mu + B - \mu')d\mu'^2, \qquad (2)$$

where B denotes the binding energy of d^*. In Eq. (2), $\rho_\Delta(\mu)$ is the mass distribution function of Δ that is given as

$$\rho_\Delta(\mu) = \frac{m^*\Gamma(\mu)}{\pi[(\mu^2 - m^{*2})^2 + m^{*2}\Gamma(\mu)^2]}, \qquad (3)$$

where m^* is the peak mass of Δ. The form of the decay width $\Gamma(\mu)$ of the Δ provided by the $\pi^+ p \rightarrow \pi^+ p$ data is

$$\Gamma(\mu) = \Gamma_0 \frac{k^3(\mu^2, m_\pi^2)[k^2(m^{*2}, m_\pi^2) + \gamma^2]}{k^3(m^{*2}, m_\pi^2)[k^2(\mu^2, m_\pi^2) + \gamma^2]}, \qquad (4)$$

where k, the momentum in the $\pi^+ p$ center-of-mass system, is given by

$$k(\mu^2, m_\pi^2) = [(\mu^2 + m_p^2 - m_\pi^2)^2/4\mu^2 - m_p^2]^{1/2}. \qquad (5)$$

The values of Γ_0 and γ are 120 and 200 MeV, respectively.

IV. TRANSITION MATRIX ELEMENT

To calculate the transition matrix elements for $pd \rightarrow pd^*$, shown typically by the diagrams given in Figs. 1 and 2, one

of the essential ingredients is the t matrix. $t_{NN\to N\Delta}$, for the transition process $NN\to N\Delta$. For this, we have taken guidance from Ref. [23]. The transition matrix is given in the distorted-wave Born approximation as

$$t_{pp\to N\Delta}=(\chi^-_{\mathbf{k_f}},\langle N\Delta^{++}|v_{tr}|NN\rangle,\chi^+_{\mathbf{k_i}}), \tag{6}$$

where v_{tr} is the $NN\to N\Delta$ transition potential that is taken as one-pion-exchange potential. In Eq. (6), χ's are the distorted waves describing the elastic scattering of the NN and the $N\Delta$ systems. It has been found in Ref. [23] that this t matrix reproduces the available experimental data very well on this reaction over a large energy range. A parametrized form of this t matrix, which is complex with a weak imaginary part, is given in Ref. [23] for calculational utility. The real part, however, resembles very much the one-pion-exchange potential. For the present calculations, instead of repeating the full calculation of the t matrix, the form that we have used is given as

$$t_{NN\to N\Delta}=V_\pi(q,\omega)[\sigma_1 S_2^+ + S_{12}(\hat{q})]\tau_1 T_2^+, \tag{7}$$

where σ and τ represent spin and isospin operators, respectively, and S and T denote, respectively, the spin and isospin transition operators that are defined as

$$\langle\sigma'|S^+(T^+)_m|\sigma\rangle=C\begin{pmatrix}\frac{1}{2} & 1 & \frac{3}{2}\\ \sigma & m & \sigma'\end{pmatrix}, \tag{8}$$

where $C(\cdots)$ denotes the Clebesch-Gordon coefficients. $S_{12}(\hat{q})$ in Eq. (7) denote the two-body noncentral operator whose form is given as

$$S_{12}(\hat{q})=3(\sigma_1\hat{q})(S_2^+\hat{q})-\sigma_1 S_2^+. \tag{9}$$

$V_\pi(\omega,\vec{q})$ in Eq. (7) is given as

$$V_\pi(\omega,\vec{q})=\frac{f_\pi f_\pi^*}{m_\pi^2}F_\pi(\omega,q)F_\pi^*(\omega,q)\frac{q^2}{\omega^2-m_\pi^2+q^2}, \tag{10}$$

where ω and $\vec{q}$ are the energy and the three-momentum transfer at the transition vertex. m_π ($\approx$139 MeV) is the mass of pion. f_π and f_π^* are the coupling constants at the πNN and $\pi N\Delta$ vertices, respectively. The magnitude of these coupling constants, which describe the pion-nucleon scattering data and Δ width well, are

$$f_\pi=1.008, \quad f_\pi^*=2.156. \tag{11}$$

The expressions of the form factors in Eq. (7), $F_\pi(\omega,q)$ and $F_\pi^*(\omega,q)$ at the πNN and $\pi N\Delta$ vertices, are taken as the same. We take those of monopole form given as

$$F_\pi(\omega,q)=F_\pi^*(\omega,q)=\frac{\Lambda_\pi^2-m_\pi^2}{\Lambda_\pi^2-\omega_\pi^2+q^2} \tag{12}$$

with the length parameter Λ_π equal to 650 MeV/c.

In the above description, for the $p\to\Delta$ excitation, we have not included the contribution of ρ exchange for this excitation. While the ρ exchange is absolutely essential to account for the $p(n,p)n$ data, it is not favored [23,24] at all by the $p(p,n)\Delta^{++}$ data. The reason for this disfavor of the ρ exchange in Δ excitation, to a certain extent, is provided by a microscopic study of the $\rho N\Delta$ vertex by Haider and Liu [25], where they find that the microscopically calculated value of the $\rho N\Delta$ coupling constant $f_{\rho N\Delta}$ is much smaller than the normally assumed value.

After fixing $NN\to N\Delta$ transition matrix we now turn to write the transition amplitude for $pd\to pd^*$. For this, we consider that the initial-state proton and deuteron are in the state of spin projection m and M_i, respectively, and the final state proton and d^* are in the state of spin projection m' and M_f, respectively. The transition amplitude for $pd\to pd^*$ can be written in terms of the transition amplitudes corresponding to direct and exchange processes as

$$\begin{aligned}T^{fi}(m,M_i,\vec{k}_i;m',M_f,\vec{k}_f)&=T_D^{fi}(m,M_i,\vec{k}_i;m',M_f,\vec{k}_f)\\&\quad-T_E^{fi}(m,M_i,\vec{k}_i;m',M_f,\vec{k}_f),\end{aligned} \tag{13}$$

where $\vec{k}_i$ and $\vec{k}_f$ denote the initial- and final-state momentum in the center-of-mass frame. The transition amplitude corresponding to a typical direct term $T_D^{fi}(m,M_i,\vec{k}_i;m',M_f,\vec{k}_f)$ can be written as

$$\begin{aligned}&T_D^{fi}(m,M_i,\vec{k}_i;m',M_f,\vec{k}_f)\\&=\sum_{m_{s_2},m_{s_3},m'_{s_2},m'_{s_3}}C\begin{pmatrix}\frac{1}{2} & \frac{1}{2} & 1\\ m_{s_2} & m_{s_3} & M_i\end{pmatrix}\\&\quad\times C\begin{pmatrix}\frac{3}{2} & \frac{3}{2} & 3\\ m'_{s_2} & m'_{s_3} & M_f\end{pmatrix}\\&\quad\times\sum_{\mu\nu}T_D^{\mu\nu}(m,m_{s_2},m_{s_3},\vec{k}_i;m',m'_{s_2},m'_{s_3},\vec{k}_f)\end{aligned} \tag{14}$$

with

$$\begin{aligned}&T_D^{\mu\nu}(m,m_{s_2},m_{s_3},\vec{k}_i;m',m'_{s_2},m'_{s_3},\vec{k}_f)\\&=\frac{1}{(2\pi)^6}I_D\int d^3p\,d^3q\,\psi^*_{d^*}(\vec{p}+\vec{q})\psi_d(\vec{q})\\&\quad\times\langle m',m'_{s_3}|V_\mu^{13}(\vec{k}_1)|m',m_{s_3}\rangle G(K)\\&\quad\times\langle m',m'_{s_2}|V_\nu^{12}(\vec{k}_2)|m,m_{s_2}\rangle,\end{aligned} \tag{15}$$

where the indices μ and ν run over the central and noncentral components of the $NN \rightarrow N\Delta$ transition potential. The momenta $\vec{k}_1$, $\vec{k}_2$, and $\vec{K}$ are related to the initial- and final-state momenta $\vec{k}_i$ and $\vec{k}_f$, respectively, as

$$\vec{k}_1 = \frac{\vec{k}_i - \vec{k}_f}{2} + \vec{p}, \quad \vec{k}_2 = \frac{\vec{k}_i - \vec{k}_f}{2} - \vec{p}, \quad \vec{K} = \frac{\vec{k}_i + \vec{k}_f}{2} + \vec{p} \tag{16}$$

with $\vec{p}$ and $\vec{p}+\vec{q}$ denoting the Fermi momentum of deuteron and d^*, respectively. The matrix elements corresponding to the central and noncentral parts of the $NN \rightarrow N\Delta$ transition potential are

$$\langle m_3, m_4 | V_C^{12}(\vec{k}_1) | m_1, m_2 \rangle = \sum_m C\begin{pmatrix} \frac{1}{2} & 1 & \frac{1}{2} \\ m_1 & m & m_3 \end{pmatrix} \sqrt{3} C\begin{pmatrix} \frac{1}{2} & 1 & \frac{3}{2} \\ m_2 & -m & m_4 \end{pmatrix} \times V_\pi(k_1, \omega_1),$$

$$\langle m_3, m_4 | V_{NC}^{12}(\vec{k}_1) | m_1, m_2 \rangle = 3\sqrt{\frac{8\pi}{15}} \sum_{m,n,M} C\begin{pmatrix} 1 & 1 & 2 \\ -m & -n & M \end{pmatrix} C\begin{pmatrix} \frac{1}{2} & 1 & \frac{1}{2} \\ m_1 & m & m_3 \end{pmatrix} \times \sqrt{3} C\begin{pmatrix} \frac{1}{2} & 1 & \frac{3}{2} \\ m_2 & n & m_4 \end{pmatrix} Y_{2M}(\hat{k}_1) V_\pi(k_1, \omega_1). \tag{17}$$

$G(K)$ denotes the propagator of the excited proton in the intermediate state. We have taken only nucleonic (neutron and proton) degrees of freedom for this excited state. I_D represents the isospin factor, expression for which can be written as

$$I_D = \sum_{m_\tau} \langle d^*(2,3) p(1) | \tau(1) T(2) | m_\tau(1) \rangle \times \langle m_\tau(1) | \tau(1) T(3) | d(2,3) p(1) \rangle, \tag{18}$$

where m_τ represent the isospin projection of the intermediate state. As we have taken the intermediate state to be either proton or neutron, m_τ can take values of $\pm\frac{1}{2}$.

The transition amplitude corresponding to a typical exchange term $T_E^{fi}(m, M_i, \vec{k}_i; m', M_f, \vec{k}_f)$, can be obtained in the same way as Eq. (14). The momentum transfers $\vec{k}_1$, $\vec{k}_2$, and $\vec{K}$ corresponding to the exchange process are to be taken as

$$\vec{k}_1 = \frac{\vec{k}_i - \vec{k}_f}{2} + \vec{q}, \quad \vec{k}_2 = \vec{k}_i + \frac{\vec{k}_f}{2} - \vec{p}, \quad \vec{K} = \frac{\vec{k}_i + \vec{k}_f}{2} - \vec{q}, \tag{19}$$

TABLE I. Various observables with respect to the depth of V_0 of Δ-Δ interacting potential. B: Binding energy of d^*, E_p: incident proton energy corresponding to peak of excitation function, μ_m: mass of d^* at which the mass distribution peaks, and θ_p: the angle of proton at which the angular distribution peaks.

V_0 (MeV)	B (MeV)	E_p (MeV)	μ_m (MeV)	θ_p (degree)
350	291	550	2134	52
400	340	450	2082	56
500	438	300	1989	64

instead of those given by Eq. (16). The isospin factor I_D in Eq. (15) is to be changed by I_E corresponding to the exchange process. The form of I_E is given as

$$I_E = \sum_{m_\tau} \langle d^*(1,3) p(2) | \tau(2) T(1) | m_\tau(1) \rangle \times \langle m_\tau(1) | \tau(1) T(3) | d(2,3) p(1) \rangle. \tag{20}$$

V. BOUND STATES

A. Deuteron

To compute the transition amplitude we need to specify the bound-state wave functions of deuteron and d^*. For these

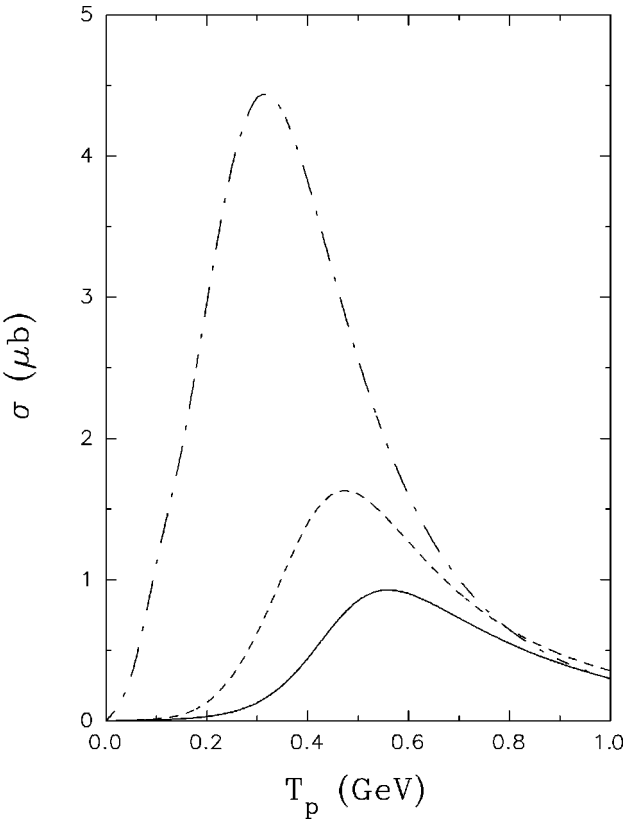

FIG. 3. Excitation function of $pd \rightarrow pd^*$ reaction. Solid, dashed, and dot-dashed curves represent, respectively, 350, 400, and 500 MeV of V_0.

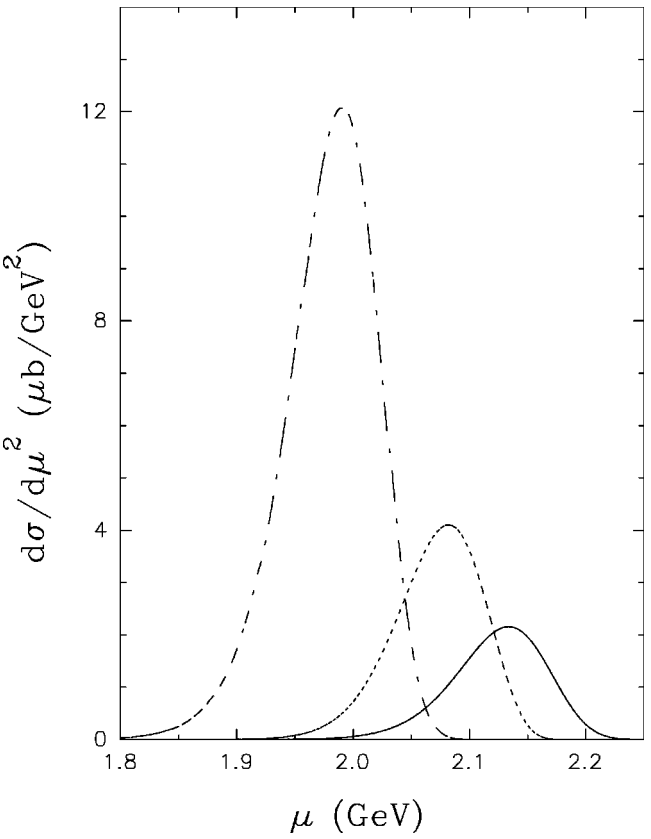

FIG. 4. Mass distribution of d^*. Solid, dashed, and dot-dashed curves represent, respectively, 350, 400, and 500 MeV of V_0.

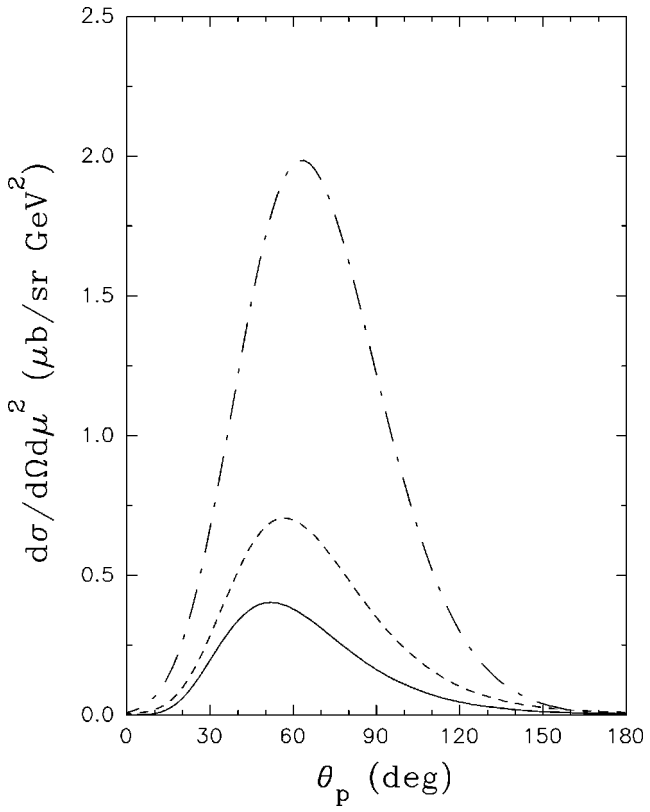

FIG. 5. Angular distribution of outgoing proton in the center-of-mass frame. Solid, dashed, and dot-dashed curves represent, respectively, 350, 400, and 500 MeV of V_0.

wave functions, we have taken only the s wave part. For deuteron we have taken Hulthen wave function that is written as

$$\psi_d(r) = \sqrt{\frac{\alpha\beta(\alpha+\beta)}{2\pi(\alpha-\beta)^2}}\,\frac{e^{-\alpha r}-e^{-\beta r}}{r} \tag{21}$$

with $\alpha = 0.2316$ fm^{-1} and $\beta = 1.268$ fm^{-1}. This wave function has been used to study pion production in proton-deuteron collisions and it describes deuteron electromagnetic form factor very well up to very large momentum transfer ($q^2 \approx 35$ fm^{-2}) [26].

B. d^*

As we have considered d^* to be a bound state of two Δ's, we calculate its wave function by solving two-body Schrodinger equation with an appropriate potential. The potential we have chosen to be is a finite circular well. The range of the potential has been taken to be 2.0 fm, whereas we have varied the depth of the potential. In our calculation we have taken three depths, namely, 350, 400, and 500 MeV. The binding energy of d^* corresponding to these potentials for Δ mass of 1232 MeV are given in the Table I. We have neglected the mild dependence of d^* binding energy on the Δ mass to calculate the width of d^* using Eq. (2).

VI. CROSS SECTIONS

We write the expression for the double differential cross sections, $d\sigma/ddtd\mu^2$ for $pd \to pd^*$ reaction as

$$\frac{d\sigma}{d\Omega d\mu^2} = \frac{k_i k_f}{\pi}\,\frac{d\sigma}{dtd\mu^2} = \frac{m_d \mu m_p^2}{4\pi^2 s}\,\frac{k_f}{k_i}\langle|T_{fi}|^2\rangle\rho(\mu^2), \tag{22}$$

where m_d, μ, and m_p denote deuteron, d^*, and proton masses, respectively, s is square of total center-of-mass energy and t is four-momentum transfer square. In Eq. (22), k_i and k_f denote initial- and final-state momenta, respectively. $\langle|T_{fi}|^2\rangle$ is the square of the transition amplitude averaged and summed over the initial- and final-state spin projections, respectively, which is written as

$$\langle|T_{fi}|^2\rangle = \frac{1}{6}\sum_{m,M_i,m',M_f} |T^{fi}(m,M_i,\vec{k}_i;m',M_f,\vec{k}_f)|^2, \tag{23}$$

where $\rho(\mu^2)$ is the mass distribution function of d^*. The expressions for other cross sections can be written as

$$\frac{d\sigma}{d\mu^2} = \int d\Omega\,\frac{d\sigma}{d\Omega d\mu^2}, \tag{24}$$

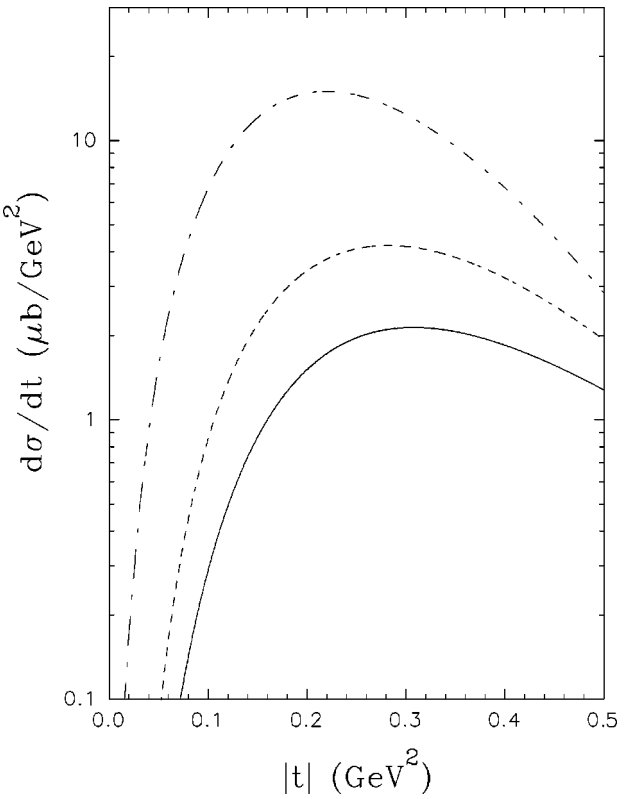

FIG. 6. t distribution of $pd \rightarrow pd^*$. Solid, dashed, and dot-dashed curves represent, respectively, for 350, 400, and 500 MeV of V_0.

$$\frac{d\sigma}{dt} = \int d\mu^2 \frac{d\sigma}{dt d\mu^2}, \tag{25}$$

$$\sigma = \int d\Omega d\mu^2 \frac{d\sigma}{d\Omega d\mu^2}. \tag{26}$$

VII. RESULTS AND DISCUSSIONS

We first calculate the excitation function for $pd \rightarrow pd^*$ reaction. For that we compute $d\sigma/d\Omega d\mu^2$ for a set of incident energy of d^* over a grid of the mass μ, and the angle θ of the outgoing proton, using Eq. (22) and the prescriptions for bound-state wave functions and d^* mass distribution as described in previous sections. The limits of θ are taken from 0° to 180° whereas those of μ is fixed by the kinematics. From this set of data we calculate the total cross section as a function of incident energy by integrating $d\sigma/d\Omega d\mu^2$ as shown in Eq. (24). The results are shown in Fig. 3. Three curves in this figure have been obtained by taking different values for the depth V_0 of the interacting potential between two Δ's forming d^*. The excitation function depends very strongly on V_0; it peaks at incident energies of 550, 450, and 300 MeV for V_0 to be 350, 400, and 500 MeV, respectively, the corresponding cross sections being 0.9, 1.6, and 4.4 μb.

We then calculate mass distribution of d^*. First, we consider the case where V_0 is 350 MeV. As in this case, the excitation function peaks around 550 MeV, we take the incident energy of proton to be 550 MeV and calculate $d^2\sigma/d\Omega d\mu^2$. We get mass distribution $d\sigma/d\mu^2$ from the double differential cross section by integration as shown in Eq. (24). We show the results in Fig. 4. In this figure, we also show that the d^* mass distribution corresponds to 400 and 500 MeV of V_0 for which the incident proton energies are 450 and 300 MeV, respectively. The mass distribution peaks at 2134, 2082, and 1989 MeV for 350, 400, and 500 MeV of V_0, respectively. Thus, we see in this simplified picture that from the d^* mass distribution, if measured, we can get some knowledge about the interacting potential of two Δ's.

We have calculated the angular distribution of the outgoing proton in center-of-mass frame for three values of V_0, namely, 350, 400, and 500 MeV. We have chosen corresponding to 350, 400, and 500 MeV of V_0, the incident proton energies and the masses of d^*, respectively, as 550, 450, and 300 MeV and 2134, 2082, and 1989 MeV. Then, we calculate the angular distribution $d^2\sigma/d\Omega d\mu^2$ corresponding to the above values of incident energy, d^* mass, and V_0. The results are shown in Fig. 5. We find that the angular distribution peaks at 52°, 56°, and 64°, respectively, for 350, 400, and 500 MeV of V_0.

In Fig. 6 we show the t (four-momentum transfer square) distribution of $pd \rightarrow pd^*$ reaction for three values of V_0. In this case too, we have chosen corresponding to 350, 400, and 500 MeV of V_0, the incident proton energies respectively as 550, 450, and 300 MeV. First we calculate, for a given value of t, $d^2\sigma/d\mu^2 dt$ for a kinematically allowed range of μ^2 determined by the incident energy and t. Then, we compute $d\sigma/dt$ by integrating this data as given in Eq. (24). The t-distribution peaks at $t = 0.31$, 0.28, and 0.22 GeV^2 for 350, 400, and 500 MeV of V_0, respectively.

VIII. SUMMARY

We have studied $pd \rightarrow pd^*$ reaction over a wide range of incident proton energy for three choices of the depth of the interacting potential between two Δ's. Our main findings are given in Table I. With the increase of the depth (V_0) of the potential the binding energy of the d^* increases, consequently we see from the mass distribution curves given in Fig. 4 that the peak mass of d^* decreases. The width of the d^* mass distribution is about 85 MeV and it remains almost same for all the three cases. The cross section too increases with increasing V_0. The peak of the excitation function, as shown in Fig. 3, also strongly depends on V_0, with increase in V_0 the peak energy of the excitation function becomes lower. On the other hand, the angle at which the angular distribution peaks depends weakly on V_0. Thus, using the results of this investigation and the data on d^* observation, it will be possible to get information regarding the nature of the interacting potential between two Δ's forming d^*.

[1] M. Lacombe, B. Loiseau, R. Vinh Mau, J. Cote, P. Pires, and R. de Tourreil, Phys. Lett. **101B**, 139 (1981).
[2] R. Machleidt, Adv. Nucl. Phys. **19**, 189 (1989).
[3] R. L. Jaffe, Phys. Rev. Lett. **38**, 195 (1977).
[4] N. K. Glendenning and J. Schaffner-Bielich, Phys. Rev. C **58**, 1298 (1998).
[5] C. W. Wong and K. F. Liu, Phys. Rev. Lett. **41**, 82 (1978).
[6] T. Goldman, K. Maltman, G. J. Stephenson, K. E. Schmidt, and F. Wang, Phys. Rev. C **39**, 1889 (1989).
[7] C. W. Wong, Phys. Rev. C **58**, 2414 (1998).
[8] D. Qing, H. Sun, and F. Wang, Phys. Rev. C **62**, 018201 (2000).
[9] C. W. Wong, Phys. Rev. C **61**, 064011 (2000).
[10] LISS (light ion spin synchroton) white paper, 1995, Indiana University Cyclotron Facility at http://www.iucf.indiana.edu/Publications/LISS.html
[11] R. Bilger *et al.*, Z. Phys. A **43**, 491 (1992); Phys. Rev. Lett. **71**, 42 (1993); **72**, 2972 (1994).
[12] R. Bilger, πN Newslett. **10**, 47 (1995).
[13] R. Bilger *et al.*, Nucl. Phys. **A596**, 586 (1996).
[14] R. Meier *et al.* πN Newslett. **13**, 234 (1997).
[15] R. Bilger *et al.*, Acta Phys. Pol. B **29**, 2415 (1998).
[16] J. Grater *et al.*, Phys. Lett. B **420**, 37 (1998); Phys. Rev. C **58**, 1576 (1998).
[17] H. Calen *et al.*, Phys. Lett. B **427**, 248 (1998).
[18] F. Lehar, in *Baryons '98*, edited by D. W. Menze and B. Ch. Metsch (World Scientific, Singapore, 1999), p. 622.
[19] CHAOS Collaboration, J. Grater *et al.*, Phys. Lett. B **471**, 113 (1999).
[20] LEPS, TAPS/A2, and PROMICE/WASA Collaboration, R. Bilger, πN Newslett. **15**, 90 (1999).
[21] CHAOS Collaboration, R. Tacik, πN Newslett. **15**, 96 (1999).
[22] U. Siodlaczek *et al.*, Eur. Phys. J. A **9**, 309 (2000).
[23] B. K. Jain and A. B. Santra, Phys. Rep. **230**, 1 (1993).
[24] V. Dmitriev, O. Sushkov, and C. Gaarde, Nucl. Phys. **A459**, 503 (1986).
[25] Q. Haider and L. C. Liu, Phys. Lett. B **335**, 253 (1994).
[26] M. P. Locher and H. J. Weber, Nucl. Phys. **B76**, 400 (1974).